


 Cite this: *RSC Adv.*, 2022, 12, 5340

# Preparation and properties of water-based acrylic emulsion-assisted flexible building tiles†

 Wu Zhang,<sup>bc</sup> Jingchen Bai,<sup>d</sup> Changlin Zhou,<sup>bc</sup> Hong Yu<sup>\*ac</sup> and Lei Wang<sup>id</sup> <sup>\*bc</sup>

The heavy and rigid appearance of conventional burnt building tiles is not suitable for a global sustainable development strategy. Flexible facing tiles with lightweight and environmental materials are highly desirable for the construction industry today. In this work, water-based polymer emulsion-assisted flexible building tiles were prepared. Based on the method of achieving post crosslinking and improving adhesion with inorganic matrix-based materials, WPAs modified with GMA and KH570 display good chemical resistance and low solvent absorption (0.132 in water and 0.289 in ethanol respectively). The optimum mechanical performance of flexible building materials prepared with WPAs can strain 1.406% and stress 1.8658 MPa. The TGA, XRD, SEM and AFM results further indicate the excellent thermal stability and compatibility of flexible building tiles. Hence, flexible building tiles prepared with WPAs can be promising building materials for construction.

 Received 4th January 2022  
 Accepted 31st January 2022

DOI: 10.1039/d2ra00045h

[rsc.li/rsc-advances](http://rsc.li/rsc-advances)

## Introduction

As one of the highly important parts of the construction industry, building tiles have been largely employed in architecture indoors and outdoors.<sup>1</sup> With the acceleration of global urbanization, there is a huge demand for building tiles. Traditional building materials are the type of clay and ceramic, which consume much energy and produce more than three wastes during the process of manufacturing.<sup>2,3</sup> Furthermore, these building tiles are heavy and highly susceptible to dislodgement, resulting in injury accidents.<sup>4</sup> Hence, instead of traditional building tiles, facing tiles with lightweight and environmental materials have become the hot topic in recent years.<sup>5</sup>

Extensive research has been performed on lightweight and environmental building materials including fly ash, amorphous silica, cigarette butts, paper-processing residues, plastic wastes, and polystyrene foams.<sup>6–9</sup> For example, Mishra and coworkers developed novel ceramic foams from inexpensive amorphous silica, the density of which decreased 89% of the theoretical values.<sup>6</sup> Mann and Brar *et al.* reported fly ash-based lightweight clay tiles and used them as radiation shielding materials.<sup>7</sup> Afzal

and Raut, in a study about sustainable building tiles, introduced waste marble powders or by-products from the paper industry to produce lightweight and environmental building materials.<sup>8,9</sup> Nevertheless, all of these building materials reduce production costs and pollution emissions to a certain extent, and the rigid appearance is not suitable for application in curved wall decoration. Consequently, the development of flexible building materials is a key direction in the current construction industry.

Due to the development of organic–inorganic hybridization science and technology, organic emulsions such as butadiene latex, neoprene latex, and acrylic copolymer emulsions have largely been employed in unburnt tiles because of their eco-friendly properties, attractive mechanical and mechanics characteristics, simple manufacturing process, and low cost.<sup>10,11</sup> Organic emulsions are a kind of polymer with hydrophilic network structures that can fill between inorganic matrix materials and serve as a binder after film-forming. Up to now, organic emulsions have been widely used in construction, bridge, ground, anti-corrosion, bonding, *etc.*<sup>12</sup> He and coworkers reviewed polymer cement materials modified by superabsorbent polymers (SAP), which concluded that the addition of SAP to cement materials could effectively solve the cracking issues during the curing and forming process.<sup>11</sup> Recently, Lee *et al.* prepared cement-based composites modified by styrene acrylic emulsion (SAE) and nitobond acrylic (AR), which could be applied as load-bearing walls with a compressive strength as high as 8.4–9.35 MPa.<sup>13</sup> However, the above-mentioned applications considered the bonding properties of the polymers and ignored the flexibility and mechanical performances of these. Extensive literature reported that organic emulsions can apply in electronics, coatings,

<sup>a</sup>Engineering Research Center of Phosphorus Resources Development and Utilization of Ministry of Education, Wuhan Institute of Technology, Wuhan 430205, China. E-mail: [yu908250@126.com](mailto:yu908250@126.com)

<sup>b</sup>College of Materials and Chemical Engineering, Key Laboratory of Inorganic Nonmetallic Crystalline and Energy Conversion Materials, China Three Gorges University, Yichang, 443002, China. E-mail: [lei.wang@ctgu.edu.cn](mailto:lei.wang@ctgu.edu.cn)

<sup>c</sup>Hubei Three Gorges Laboratory, Yichang, Hubei, 443007, China

<sup>d</sup>Hubei Yaomei Soft Porcelain Co., Ltd, Yichang, 443500, China

† Electronic supplementary information (ESI) available: Properties of WPAs with different content of GMA or KH570, <sup>1</sup>H NMR spectrum of WPAs. See DOI: 10.1039/d2ra00045h



packaging, and so on.<sup>14–16</sup> Up to now, part of commercially available acrylic emulsions (*e.g.* architectural coatings, lacquer) are introduced to fabricate flexible building tiles. Most of them are based on existing commercialized emulsions for direct industrial applications. As a result, the development of flexible building tiles mainly focuses on the formulation study. However, the essential roles of the organic emulsions in the flexible building tiles are usually neglected. In order to fabricate industrial flexible building tiles, constructing the hard/soft latex blend-based flexible building tiles is the main solution. However, the poor weatherability of the blend systems makes it necessary to adjust the formula frequently. Moreover, the poor compatibility between the commercially available emulsions and the inorganic materials induces the need to add a large proportion of the commercially available emulsions, resulting in increasing the whole production costs.

To address the above-mentioned problems of commercially available products, this paper focuses on the preparation of water-based polyacrylate resins (WPAs) with excellent comprehensive properties (including good flexibility, low water, solvent absorption, short drying time, and excellent mechanical performances). It should note that the basic building blocks such as types and addition amounts of vinyl monomers and glass transition temperature ( $T_g$ ) largely influenced the properties of the membrane. Furthermore, the investigation about the effect of WPA was also taken into account. Through single-factor variable regulation, the promising supporting materials were screened and applied in producing flexible building tiles (Scheme 1).

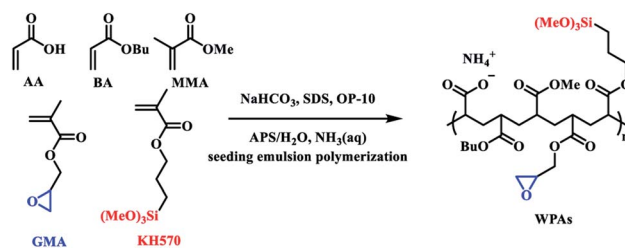
## Results and discussion

### Design principle of WPAs

To prepare flexible building tiles, the efficient combination of inorganics and organics is the key consideration for the design of WPAs. Due to the larger proportion and the inertness of inorganic sections, the modification strategies including achieving post crosslinking and improving the adhesion with inorganic matrix materials were taken into account.<sup>20–22</sup> As a result, KH570 and GMA were chosen as functional monomers to achieve the purpose. The synthetic route of WPAs is illustrated in Scheme 2. The epoxy group in the molecular structure of GMA significantly improved the adhesion with the inorganic



Scheme 1 Schematic diagram of flexible building tiles prepared by WPAs.



Scheme 2 Synthetic route of WPAs.

powder, and an amine curing agent was added to realize post crosslinking in the process of preparing flexible building tiles.<sup>23,24</sup> The  $\text{SiOCH}_3$  group in KH570 could transform into  $\text{Si-OH}$  during the hydrolysis process, which enhanced the combining ability with exposed hydroxyl groups on the surface of inorganic powder and increased the crosslinking degree of composite materials.<sup>25,26</sup> The BA and MMA were selected as soft monomers and hard monomers respectively, which would regulate the performance of WPAs by changing the proportion. Based on the above-mentioned design strategy, the WPAs for flexible building tiles were prepared.

### Characteristics of WPAs

The FTIR spectra were employed to study the change in the characteristic peaks in GMA, KH570, and WPAs (Fig. 1a). As depicted in Fig. 1b, the characteristic peak around  $1724\text{ cm}^{-1}$

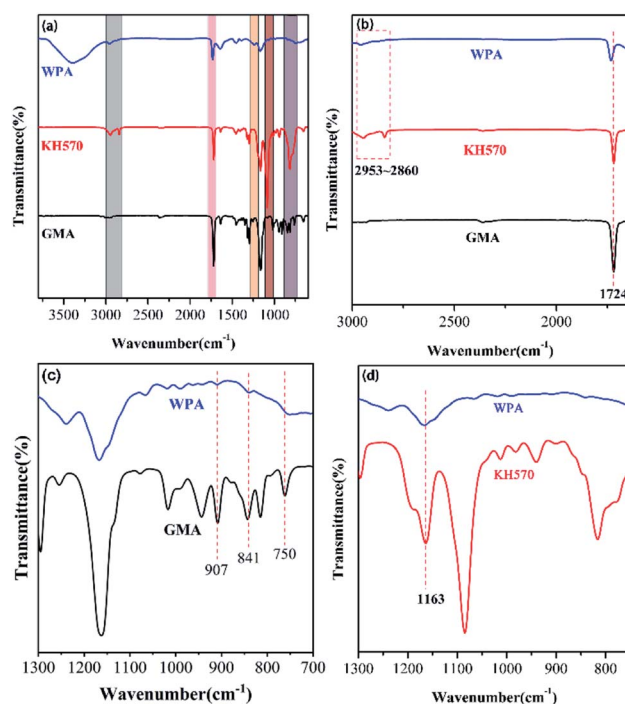


Fig. 1 (a) FTIR spectra of GMA, KH570, and WPA. (b) Enlarged FTIR spectra of GMA, KH570, and WPA ranging from  $3000\text{ cm}^{-1}$  to  $1600\text{ cm}^{-1}$ . (c) Enlarged FTIR spectra of GMA and WPA ranging from  $1400\text{ cm}^{-1}$  to  $700\text{ cm}^{-1}$ . (d) Enlarged FTIR spectra of KH570 and WPA ranging from  $1300\text{ cm}^{-1}$  to  $750\text{ cm}^{-1}$ .



attributed to carbonyl group (C=O) stretching that appeared in both spectra. Apart from that, the peaks located at  $2953\text{ cm}^{-1}$  and  $2860\text{ cm}^{-1}$  existed in both spectra, assigned to the stretching vibrations of C–H and  $\text{CH}_2$ , respectively.<sup>27,28</sup> Furthermore, the typical epoxy peaks at  $750\text{ cm}^{-1}$ ,  $841\text{ cm}^{-1}$ , and  $907\text{ cm}^{-1}$  were recognized in both GMA and WPAs (Fig. 1c).<sup>23,24,29</sup> Moreover, the stretching vibration peak of Si–O at  $1163\text{ cm}^{-1}$  was examined in KH570 and WPAs respectively (Fig. 1d).<sup>25,26,30</sup>

We also conducted the  $^1\text{H}$  NMR test to characterize the structure of WPAs. As illustrated in Fig. S1,† the chemical shifts of hydrogen atoms in WPAs were located around  $\delta = 0\text{--}4.09$  ppm. The peaks at  $\delta = 1.63$  and  $3.68$  belong to the characteristic peak of (– $\text{CH}_2$ –) and (– $\text{OCH}_3$ ) after the reaction of double bond groups participating in polymerization, respectively. Moreover, the peaks at  $\delta = 4.09$  and  $3.34$  were attributed to the side chain of (–Si– $\text{OCH}_3$ ) in KH570 and (– $\text{CH}_2$ –) in GMA, respectively. These results highly indicate that the WPAs were synthesized as expected.

### Effect of GMA

The effect of GMA on WPAs was first evaluated. As shown in Table S1,† the viscosity and particle sizes of WPAs significantly increase according to the increase in GMA content. The main reason for this phenomenon might be a partial ring-opening reaction that occurred in the epoxy unit under the high-temperature reaction system, which induced the increasing intermolecular hydrogen bonding.<sup>31</sup> Furthermore, the unnecessary side reactions would cause adhesion between emulsion particles and increase the particle sizes respectively. As a result, the content of GMA should not be higher than 5 wt%, and the viscosity and particle sizes of WPAs were  $752\text{ mPa s}$  and  $216\text{ nm}$ , which were suitable for the preparation of flexible building tiles.

The chemical resistance and absorption experiments were subsequently conducted. As displayed in Table 1, the WPA films exhibited excellent chemical resistance in acid, alkali, and water media. With the addition of GMA, more crosslinking points are provided for polymerization, which improved the content of crosslinked network structure. Consequently, the chemical resistance of the WPA films was significantly improved. However, the introduced water-absorbent groups would dramatically influence the polymerization stability and decrease the film-forming ability of WPAs with the high content of GMA. Consequently, the content of GMA would significantly influence the comprehensive performance of WPA films. While

the dosage of GMA is 2 wt%, the WPA films in run 2 reached the lowest minimum value, which was 0.157 and 0.354 respectively. These results highly proved that the optimal dosage of GMA is 2 wt%.

As a kind of flexible building material, the tensile stress-strain property was further evaluated. Fig. 2 depicts the stress-strain curves of flexible building tiles prepared by WPAs with different GMA contents. The elongation at break increased from 0.933 to 1.207% with the increase in GMA content (1–2 wt%), and the tensile strength rose from 0.509 to 1.093 MPa respectively. With the further increase in the content of GMA (3–5 wt%), the elongation at break and tensile strength dramatically decreased to 0.809% and 0.663 MPa respectively. This suggested that the introduction of GMA significantly improved the mechanical properties of flexible building materials. However, the large amount of GMA greatly increased the viscosity and particle sizes of WPAs induced by the ring-opening reaction in the epoxy units during the polymerization process. The stability and filler dispersion of emulsions were dramatically decreased and accompanied by the worse mechanical

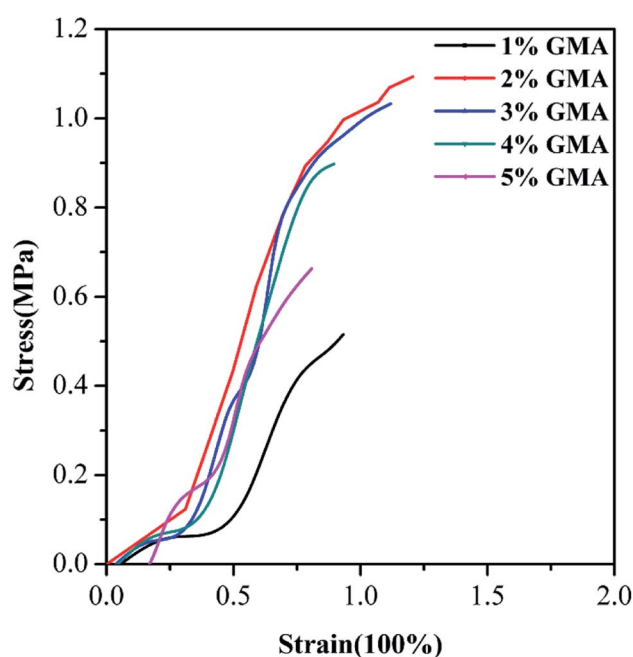


Fig. 2 Stress–strain curves of flexible building tiles prepared with WPAs having different GMA contents.

Table 1 Chemical resistance and absorption of WPA films with different GMA contents<sup>a</sup>

Runs	GMA%	Acid <sup>b</sup>	Alkali <sup>b</sup>	Ethanol <sup>b</sup>	Toluene <sup>b</sup>	Cold water <sup>b</sup>	Hot water <sup>b</sup>	Water absorption	Ethanol absorption
1	1	1	2	3	3	2	2	0.18	0.405
2	2	1	1	2	2	1	2	0.157	0.354
3	3	1	2	3	4	2	2	0.277	0.49
4	4	1	2	3	4	3	3	0.289	0.509
5	5	1	3	4	4	3	3	0.307	0.517

<sup>a</sup> KH570 content = 3 wt%, theoretical  $T_g = 0\text{ }^\circ\text{C}$ . <sup>b</sup> Chemical resistance: “1” = no effect; “2” = slight whitening; “3” = whitening, “4” = blistering, “5” = dissolution.



properties of flexible building tiles. As a result, the suitable GMA content was 2 wt%.

### Influence of KH570

The effect of another important variable (KH570) was also evaluated. The performance of WPAs is displayed in Table S2,<sup>†</sup> and the viscosity and particle sizes of WPAs dramatically increased followed by the increase in the amount of KH570. Due to the SiOCH<sub>3</sub> group in KH570, hydrolysis occurred easily and induced the larger seed during the polymerization process.<sup>30</sup> The viscosity and particle sizes of WPAs increased from 89 to 893 mPa s and 76 to 246 nm respectively. More seriously, the emulsions were not stable while the KH570 content exceeded 5%.

The properties of WPA films influenced by the amount of KH570 were subsequently discussed. Table 2 displays the chemical resistance and absorption of WPA films in different media. The films exhibit excellent chemical resistance in media including acid, ethanol, and water. In general, the comprehensive performance of WPA films showed an increasing trend at first and then a decreasing trend. The optimal KH570 amount was 2 wt%, for which the water and ethanol absorption was 0.115 and 0.378 respectively. The introduction of KH570 significantly increased the cross-linking degree of WPAs to a certain extent. However, the large amount of KH570 largely raised the hydrolysis degree, which induced the larger seed and adhesion between emulsion particles. Consequently, the polymerization stability of WPAs was reduced.

As displayed in Fig. 3, the mechanical properties of flexible building tiles prepared by WPAs with different KH570 contents were increased in lower addition (1–2 wt%) and then decreased in higher ones (3–5 wt%), which was in accordance with the chemical resistance results. The maximum elongation at break and tensile strength was 1.742% and 1.6272 MPa respectively when the addition of KH570 was 2 wt%, suggesting that KH570 could efficiently improve the comprehensive performance of flexible building tiles by increasing the cross-linking degree. However, the larger amount of KH570 significantly raised the hydrolysis degree during the polymerization process. Furthermore, the seed monomers tend to aggregate and affect the stability of flexible building tiles prepared by WPAs. Hence, the optimum addition of KH570 was 2 wt%.

### Impact of $T_g$

As a kind of copolymerized polymer, the glass transition temperature ( $T_g$ ) determined their basic properties.<sup>32</sup> According

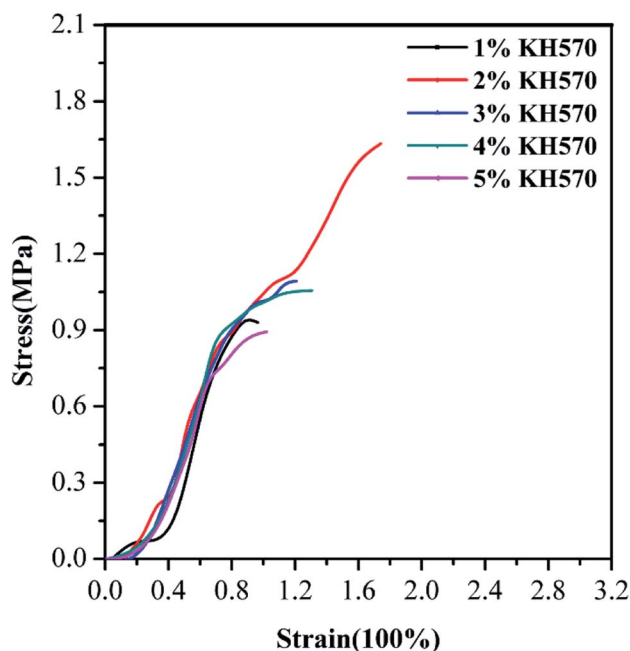


Fig. 3 Stress–strain curves of flexible building tiles prepared by WPAs with different KH570 contents.

to the Fox equation,  $T_g$  was regulated by adjusting the proportion of soft and hard monomers.<sup>33</sup> Table 3 presents the basic properties of WPAs with different  $T_g$  values. The chemical resistance and absorption were significantly increased with the increase in  $T_g$ . However, the brittleness of the films decreased under a high  $T_g$  value.<sup>34</sup> For flexible building material applications, the promising WPAs with suitable  $T_g$  were examined.

Fig. 4 shows the mechanical properties of flexible building tiles prepared by WPAs with different  $T_g$  values by tensile testing. The  $T_g$  value of WPAs significantly affected the mechanical properties of the flexible building tiles. It could obviously observe that with the increase in  $T_g$ , the strain decreased from 3.186 to 1.107%, and the stress increased from 0.891 to 2.314 MPa respectively. The reinforcement of the tensile strength was attributed to the larger cross-link density of WPAs with higher  $T_g$ . By contrast, the lower  $T_g$  value endowed the films with better flexibility. However, the elongation at break and tensile strength of flexible building tiles was comprehensively considered. The flexible building tiles were too soft for construction when prepared by lower  $T_g$  WPAs and

Table 2 Chemical resistance and absorption of WPAs film with different KH570 contents<sup>a</sup>

Runs	KH570%	Acid <sup>b</sup>	Alkali <sup>b</sup>	Ethanol <sup>b</sup>	Toluene <sup>b</sup>	Cold water <sup>b</sup>	Hot water <sup>b</sup>	Water absorption	Ethanol absorption
6	1	2	3	2	3	2	2	0.132	0.459
7	2	2	3	2	3	1	2	0.115	0.378
3	3	2	2	2	3	1	2	0.172	0.476
8	4	2	3	3	4	1	3	0.237	0.489
9	5	2	3	3	4	1	2	0.196	0.351

<sup>a</sup> GMA content = 2 wt%, theoretical  $T_g = 0^\circ\text{C}$ . <sup>b</sup> Chemical resistance: “1” = no effect; “2” = slight whitening; “3” = whitening, “4” = blistering, “5” = dissolution.



Table 3 Chemical resistance and absorption of WPAs films with different  $T_g$  values<sup>a</sup>

Runs	Theoretical $T_g$	Acid <sup>b</sup>	Alkali <sup>b</sup>	Ethanol <sup>b</sup>	Toluene <sup>b</sup>	Cold water <sup>b</sup>	Hot water <sup>b</sup>	Water absorption	Ethanol absorption
10	-10 °C	3	3	4	5	3	2	0.358	0.663
11	-5 °C	3	3	3	4	2	2	0.244	0.516
7	0 °C	2	3	2	3	1	2	0.115	0.378
12	5 °C	2	2	2	3	1	1	0.132	0.289
13	10 °C	1	1	1	2	1	1	0.100	0.226

<sup>a</sup> GMA content = 2 wt%, KH570 content = 2 wt%. <sup>b</sup> Chemical resistance: "1" = no effect; "2" = slight whitening; "3" = whitening, "4" = blistering, "5" = dissolution.

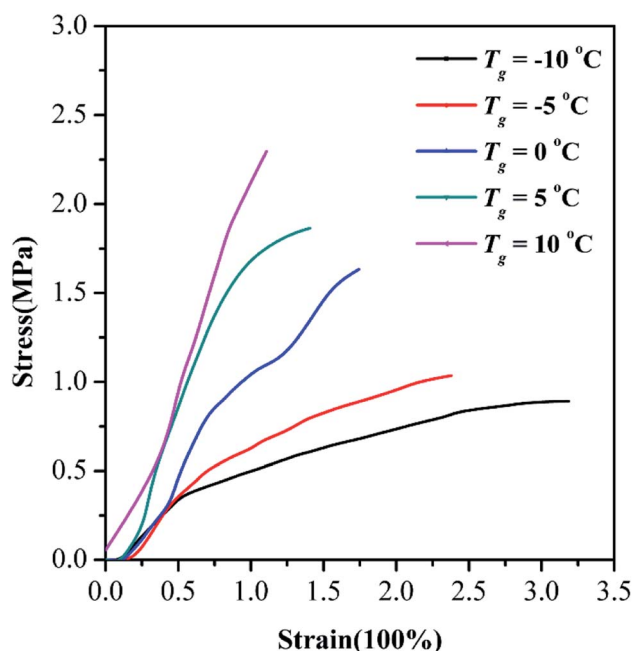


Fig. 4 Stress-strain curves of flexible building tiles prepared by WPAs with different  $T_g$  values.

too hard to break easily when prepared by the higher ones. Furthermore, the threadlike structures of WPAs would bring weakness of heat-adhesive and cold brittleness. Consequently, the optimum  $T_g$  value of WPAs for flexible building tiles was 5 °C, the elongation at break and tensile strength was 1.406% and 1.8658 MPa, respectively.

### Thermal stability analysis

The thermal stability of WPA films and flexible building tiles was further investigated by TGA.<sup>35</sup> The TGA curves are displayed in Fig. 5, and the various weight losses corresponding to the decomposition temperature are summarized in Table 4. As shown in Fig. 5a and Table 4,  $T_{5\%}$  and  $T_{10\%}$  of WPA films in run 12 were about 320.9 °C and 365.9 °C, and those of the control group were 312.9 °C and 362.9 °C respectively. This suggested the excellent thermal stability of WPA films, which was more suitable than the commercial one. Fig. 5b and Table 4 also depict the thermal stability of flexible building tiles prepared by WPAs, which started degrading at 250.4 °C and the value of  $T_{5\%}$

was 387.9 °C, 15.4 °C and 18 °C higher than those of commercial group, proving the excellent stability at high temperatures. These indicated the more homogeneous structure in tiles prepared by WPAs in run 12. Due to the larger proportion of inorganic materials, there was 6.26% weight loss over the range of 0–497.3 °C. These results highly demonstrated that the prepared flexible building tiles possessed excellent thermal stability and a great potential for practical applications.

### X-Ray diffraction analysis

To further study the mechanism behind the excellent properties of flexible building tiles assisted by WPAs, the XRD experiments were conducted. Fig. 6 depicts the XRD test results for the commercial tiles and the tiles prepared with WPAs in run 12 with or without the curing agent. The diffraction picks at  $2\theta = 23.2^\circ$ ,  $29.6^\circ$ ,  $39.6^\circ$ ,  $43.4^\circ$ , and  $48.6^\circ$ , corresponding to the characteristic peaks of stone dust and calcium powder ( $\text{CaCO}_3$ , JCPDS no. 47-1743) in tiles. The commercial emulsions and WPA in run 12 without the curing agent depict negligible influence on the crystallinity of inorganic matrix materials, which suggested that there was no interaction between inorganic materials and organic emulsions. By contrast, the intensity of picks at  $2\theta = 29.6^\circ$  in the prepared tiles by WPAs in run 12 within the curing agent was dramatically decreased and the peak spacing was larger than that of other groups, which was attributed to the cross-linked WPA films on the surface of inorganic particles and enhanced the amorphous degree of tiles.<sup>36</sup> As a result, the performance of the prepared tiles was significantly enhanced.

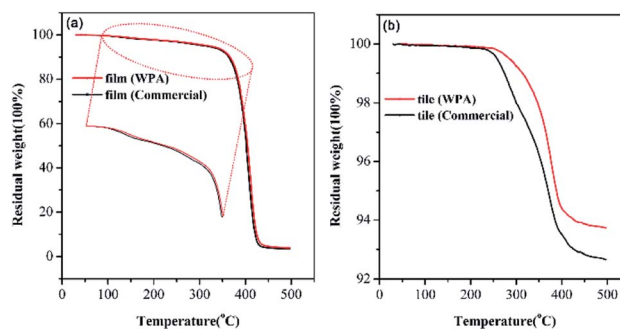


Fig. 5 TGA curves of films (a) and flexible building tiles (b).



Table 4 Main decomposition temperature of the WPA film and flexible building tiles

materials	$T_{5\%}/^{\circ}\text{C}$	$T_{10\%}/^{\circ}\text{C}$	$T_{\text{onset}}/^{\circ}\text{C}$	$T_{\text{inflection}}/^{\circ}\text{C}$	$T_{\text{end}}/^{\circ}\text{C}$
Film (WPA in runs 12)	320.9	365.9	192.9	440.0	497.5
Film (commercial)	312.9	362.9	184.9	430.0	497.2
Tile (WPA in runs 12)	387.9	—	250.4	450.3	497.3
Tile (commercial)	369.9	—	235.0	450.3	497.4

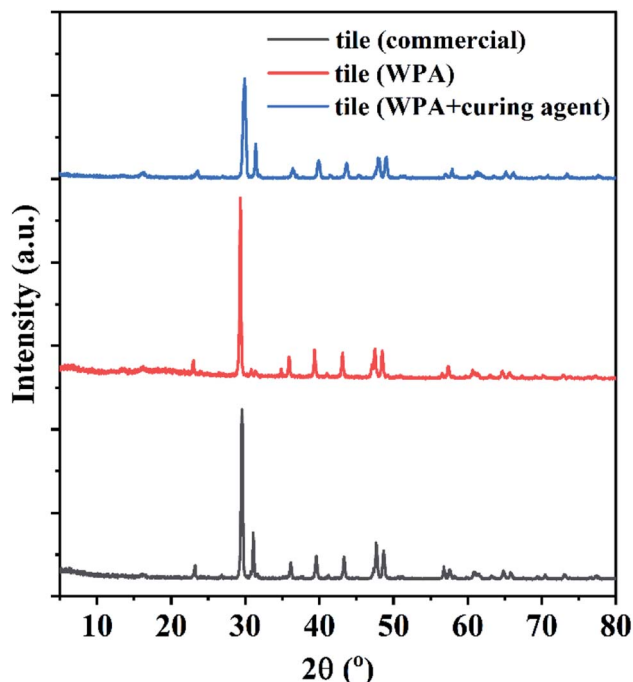


Fig. 6 XRD spectra of tiles prepared with commercial emulsions and the WPA in run 12 with or without the curing agent.

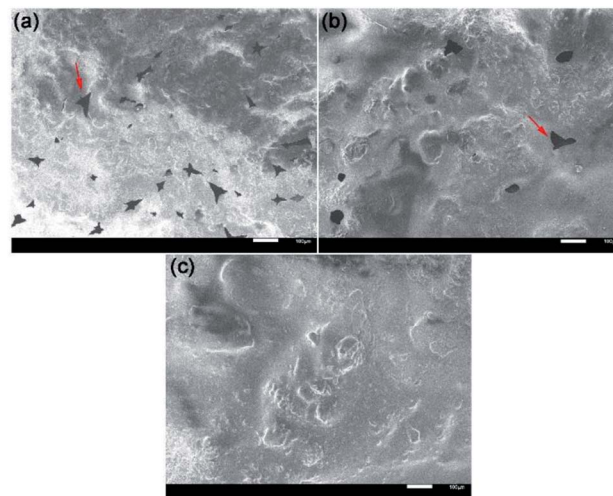
### Morphological analysis

The morphology of flexible building tiles was further investigated by SEM.<sup>37</sup> To prove the enhanced compatibility by adding the WPAs, commercial emulsions (Shanghai Bao Li Jia Chemical Co., Ltd) were used as the control group. As illustrated in Fig. 7a, a clear two-phase structure was observed, which indicated the weak interfacial adhesion between organic films and inorganic-based materials. Compared with the commercial tiles, the degree of the phase separation in the tiles prepared by WPAs in run 12 was significantly decreased, suggesting the GMA and KH570 modified strategies could dramatically enhance the binding affinity with the inorganic particles (Fig. 7b). Notably, the smooth and homogeneous surface with no cavitation was formed in Fig. 7c, which attributed to the cross-linked phenomenon that occurred on the surface of inorganic particles during the film forming process. These results strongly suggested that the modification strategies for WPAs including achieving post crosslinking and improving the adhesion with inorganic-based materials could significantly improve its compatibility and dispersibility.

We further conducted the AFM experiments to explore the two-phase mixing degree between organic emulsions and inorganic particles. The surfaces of all tiles consisted of many peaks and valleys, which are shown by bright regions and dark regions in all AFM images, respectively. As depicted in Fig. 8a and d, a large proportion of aggregates were formed in tiles prepared by the commercial emulsions, which attributed to the poor compatibility between the commercial emulsions and inorganic particles and induced the aggregation of inorganic particles during the drying process. By contrast, the AFM images in Fig. 8b and e show that the surface fluctuations were decreased and the proportion of aggregates was reduced, indicating the good compatibility between the WPAs in run 12 and inorganic particles. Moreover, the surface fluctuations were further reduced after adding the curing agent to the mixture system, which could achieve post crosslinking on the surface of inorganic particles. The fuzziness of the boundary in Fig. 8c and f could obviously observe the good interfacial combination between organic films and inorganic particles. These results highly proved that the prepared WPAs displayed a great potential for preparing flexible building tiles.

### Properties of flexible building tiles

As expected, the flexible building tiles were successfully prepared. As illustrated in Video S1,<sup>†</sup> the flexible building tiles exhibited excellent flexibility that could be arbitrarily bent. The

Fig. 7 SEM images of tiles prepared with commercial emulsions (a), WPA in run 12 without any curing agent (b), and WPA in run 12 with a curing agent (c). Scale bar: 100  $\mu\text{m}$ .

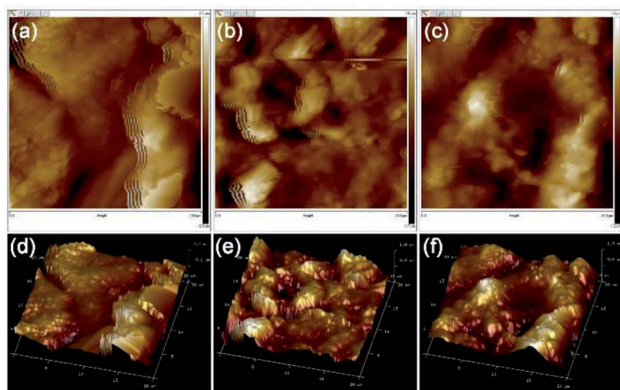


Fig. 8 Two-dimensional (a–c) and corresponding three-dimensional (d–f) AFM images of tiles prepared by commercial emulsions, WPA in run 12 without any curing agent, WPA in run 12 with a curing agent.

properties of flexible building tiles were studied and presented in Table 5. The results indicated that the flexible building tiles displayed the thin thickness (2 mm) and the lightweight ( $1.8 \text{ kg m}^{-2}$ ). Moreover, the water absorption of the flexible building tiles was lower to  $0.95 \text{ g m}^{-2} \text{ h}^{-1}$  and the anti-freezing properties of these could undergo 73 freeze-thaw cycles ( $-30$ – $20 \text{ }^\circ\text{C}$ ) respectively. Both results indicated the excellent comprehensive performance of the flexible building tiles and could serve as a kind of promising building material for construction.

## Experimental

### Materials

Glycidyl methacrylate and methacrylic propyl trimethoxyl silane were purchased from Aladdin Biochemical Technology Co., Ltd. Acrylic acid, methyl methacrylate, ammonia, and butyl acrylate were obtained from Macklin Inc. Ammonium persulphate and sodium bicarbonate were offered by Adamas Reagent, Ltd. Sodium lauryl sulfonate (SDS) and OP-10 were supplied by Sinopharm Chemical Reagent Co., Ltd. Polyether amine curing agent (D-230) was obtained from BASF Corporation. Commercial acrylic emulsions BLJ-555, calcium powder (600 mesh), fiberglass, stone dust (120–160 mesh), and hypromellose were received from Hubei Yaomei Soft Porcelain Co., Ltd. All the reagents were directly utilized without further purification unless there is a special requirement.

### Synthesis of water-based polyacrylate resins (WPAs)

According to the method reported in the literature, seeding emulsion polymerization was introduced for the synthesis of

WPAs.<sup>17,18</sup> The process of polymerization was conducted in a 250 mL three-necked flask equipped with a thermometer and a constant pressure dropping funnel (one for adding pre-emulsion, another for feeding the solution of initiator), and placed in the water bath. First, 10 wt% of pre-emulsion was taken as the seed and then half of the mixed emulsifier was added into the flask. After the reaction mixture was heated to around  $80 \text{ }^\circ\text{C}$ ,  $1/3$  of the initiator solution was added drop by drop in 30 min. Second, the last pre-emulsion and initiator solution were added separately in 150 min. The reaction system was then maintained at  $85 \text{ }^\circ\text{C}$  for further 1 h. After that, the system was cooled down to around  $50 \text{ }^\circ\text{C}$ , a certain amount of ammonia was added to regulate the pH to 7–8, and the heat was maintained for further 15 min. Finally, the emulsion was filtered through a 300 mesh filter cloth to separate the gel section and the WPAs were successfully synthesized.

### Preparation of flexible building tiles

Flexible building tiles were prepared as follows: 44.4 g stone dust, 29.6 g calcium powder, 11.1 g WPAs, a certain amount of curing agent, 0.062 g fiberglass, and 0.034 g hypromellose were mixed with  $14.8 \text{ g H}_2\text{O}$  to a 250 mL open-end vessel and stirred at a rate of 800 rpm for 15 min. The obtained slurry was encapsulated in a  $23.5 \text{ cm} \times 6 \text{ cm} \times 2 \text{ cm}$  silica gel mold and then placed in an oven for 4 h at  $75 \text{ }^\circ\text{C}$ . The flexible building tiles were obtained after demoulding.

### Characterization

The thin films on flat tin plates were obtained by drying the wet film (50 mm) for 1 day at room temperature. The chemical resistance in different environments including toluene, methanol, ethanol, and water was conducted according to relevant methods in ISO 2812-1:1993. The drying time of the thin films was adjusted following the Chinese National Standard of GB/T 1728-1979.<sup>19</sup> The water or solvent absorption of WPA films was conducted by the following methods:  $25 \text{ mm} \times 25 \text{ mm} \times 1 \text{ mm}$  dry films were immersed in water or ethanol and the initial weight ( $W_0$ ) was recorded. After 8 days, the films were removed from the solution, dried, and weighed ( $W_1$ ). The water or ethanol absorption was calculated based on the following formula:

$$\text{Absorption ratio (\%)} = (W_0 - W_1)/W_1 \times 100$$

The average particle size of WPAs was measured using a Nano-ZS laser particle sizer (Malvern, UK). The FTIR spectra of the samples were conducted using a Fourier transform instrument (PE, USA). The glass transition temperature ( $T_g$ ) and thermal stability of the samples were performed using an STA 449 F5 simultaneous thermal analyzer (NETZSCH, Germany) at a heating rate of  $10 \text{ K min}^{-1}$  ranging from  $30 \text{ }^\circ\text{C}$  to  $500 \text{ }^\circ\text{C}$  in a nitrogen atmosphere. The tiles were scanned using a Bruker D2 PHASER XRD analyzer. The scanning angle was  $10$ – $70^\circ$ , and the scanning rate was  $4^\circ \text{ min}^{-1}$ . The AFM experiments were conducted using an Innova atomic force microscope (Bruker,

Table 5 Properties of flexible building tiles

Properties	Testing standards	Tiles
Thickness	JC/T 2219-2014	2 mm
Weight	JC/T 2219-2014	$1.8 \text{ kg m}^{-2}$
Water absorption	GB/T17146-1997	$0.95 \text{ g m}^{-2} \text{ h}^{-1}$
Anti-freeze	GB/T 3810.12-2006	73 cycles
Anti-pollution	GB/T 3810.14-2006	Level 4



USA).  $^1\text{H}$  NMR spectra were measured using a Bruker 400 MHz NMR system with  $\text{CDCl}_3$ . Morphologies of flexible building tiles were studied using a JSM-7500F scanning electron microscope system (JEOL, Japan).

Tensile specimens were cut using a dumbbell cutter and then evaluated using an Instron 5567 A under ambient temperature at a tensile rate of  $30\text{ mm min}^{-1}$ . Each sample was measured for at least 4 specimens, took the average value, and recorded the tensile strength.

The apparent performance of flexible building tiles was conducted by the Chinese Industry Standard JC/T 2219-2014. The water absorption of the flexible building tiles was carried out followed by the Chinese National Standard of GB/T17146-1997. The anti-pollution and anti-freezing characteristics of the flexible building tiles were followed by the method in the Chinese National Standard of GB/T 3810.14-2006.

## Conclusions

In summary, we have developed a novel type of WPA based on the strategies of achieving post crosslinking and improving the adhesion with inorganic-based materials and applied as supporting materials for fabricating flexible building tiles. Single-factor experimental results show that GMA, KH570, and  $T_g$  can significantly affect the properties of WPA films and then influence the performance of flexible building tiles. The TGA results indicated that the flexible building tiles prepared with WPAs display excellent thermal ability. The morphological analysis also indicates uniform dispersion of WPAs in inorganic-based materials that assist in giving good properties including water absorption, anti-freezing, and anti-pollution. Thus, the excellent outcomes of the flexible building tiles prepared by WPAs indicate a great potential for green buildings. This work will provide a new insight for developing flexible building materials in the future.

## Conflicts of interest

There are no conflicts to declare.

## Acknowledgements

All authors acknowledge the support from Open Project of Engineering Research Center of Phosphorus Resources Development and Utilization of Ministry of Education (LKF201906) and the 111 Project of Hubei Province (No. 2018-19-1).

## Notes and references

- 1 A. Sev, *Sustain. Dev.*, 2009, **17**, 161–173.
- 2 P. Block, A. Schlueter, D. Veenendaal, J. Bakker, M. Begle, I. Hischer, J. Hofer, P. Jayathissa, I. Maxwell, T. MéndezEchenagucia, Z. Nagy, D. Pigram, B. Svetozarevic, R. Torsing, J. Verbeek, A. Willmann and G. P. Lydon, *J. Build. Eng.*, 2017, **12**, 332–341.
- 3 I. Z. Bribián, A. V. Capilla and A. A. Usón, *Build. Environ.*, 2011, **46**, 1133–1140.
- 4 W.-L. Hsu, C.-C. Liu, Y.-C. Shiau, C.-L. Wang and W.-C. Lin, *Sensor. Mater.*, 2019, **31**, 1071–1081.
- 5 Y. Z. Meng, T.-C. Ling and K. H. Mo, *Conserv. Recy.*, 2018, **138**, 298–312.
- 6 S. Mishra, R. Mitra and M. Vijayakumar, *J. Eur. Ceram. Soc.*, 2008, **28**, 1769–1776.
- 7 H. S. Mann, G. S. Brar and G. S. Mudahar, *Phys. Chem.*, 2016, **127**, 97–101.
- 8 Q. Afzal, S. Abbas, W. Abbass, A. Ahmed, R. Azam and M. R. Riaz, *Constr. Build. Mater.*, 2020, **231**, 117190.
- 9 S. P. Raut, R. Sedmake, S. Dhunde, R. V. Ralegaonkar and S. A. Mandavgane, *Constr. Build. Mater.*, 2012, **27**, 247–251.
- 10 H. L. Jin, J. Li, J. Iocozzia, X. Zeng, P.-C. Wei, C. Yang, N. Li, Z. P. Liu, H. He, T. J. Zhu, J. C. Wang, Z. Q. Lin and S. Wang, *Angew. Chem. Int. Edit.*, 2019, **58**, 15206–15226.
- 11 Z. M. He, A. Q. Shen, Y. C. Guo, Z. H. Lyu, D. S. Li, X. Qin, M. Zhao and Z. L. Wang, *Constr. Build. Mater.*, 2019, **225**, 569–590.
- 12 Y. F. Zuo, J. H. Xiao, J. Wang, W. J. Liu, X. G. Li and Y. Q. Wu, *Constr. Build. Mater.*, 2018, **171**, 404–413.
- 13 C. C. Lee and M. A. R. Azman, *Mater. Today Proc.*, 2020, DOI: 10.1016/j.matpr.2020.09.534.
- 14 L.-C. Jia, C.-G. Zhou, W.-J. Sun, L. Xu, D.-X. Yan and Z.-M. Li, *Chem. Eng. J.*, 2020, **384**, 123368.
- 15 J. Zhao, X. F. Wang, Y. Q. Xu, P. W. He, Y. Si, L. F. Liu, J. Y. Yu and B. Ding, *ACS Appl. Mater. Interfaces*, 2020, **12**, 15911–15918.
- 16 T. H. Zhong, M. P. Wolcott, H. Liu and J. W. Wang, *Carbohydr. Polym.*, 2019, **226**, 115276.
- 17 L. Scarabelli, M. Schumacher, D. Jimenez de Aberasturi, J. P. Merkl, M. Henriksen-Lacey, T. Milagres de Oliveira, M. Janschel, C. Schmidtke, S. Bals and H. Weller, *Adv. Funct. Mater.*, 2019, **29**, 1809071.
- 18 X. T. Yu, Y. J. Sun, F. X. Liang, B. Y. Jiang and Z. Z. Yang, *Macromolecules*, 2018, **52**, 96–102.
- 19 L. Wang, Y. A. Zhu and J. Q. Qu, *Prog. Org. Coat.*, 2017, **105**, 9–17.
- 20 G. Tillet, B. Boutevin and B. Ameduri, *Prog. Polym. Sci.*, 2011, **36**, 191–217.
- 21 Z. Liang, J. T. Zhu, F. Q. Li, Z. M. Wu, Y. J. Liu and D. Xiong, *Prog. Org. Coat.*, 2021, **150**, 105972.
- 22 A. Yumashev and A. Mikhaylov, *Polym. Composites*, 2020, **41**, 2875–2880.
- 23 M. Y. Shang, Y. J. Wu, B. Q. Shentu and Z. X. Weng, *Ind. Eng. Chem. Res.*, 2019, **58**, 12650–12663.
- 24 Z. S. Pour, M. Ghaemy, S. Bordbar and H. Karimi-Maleh, *Prog. Org. Coat.*, 2018, **119**, 99–108.
- 25 W. B. Liao, H. P. Teng, J. Q. Qu and T. Masuda, *Prog. Org. Coat.*, 2011, **71**, 376–383.
- 26 J. H. Zhou, J. J. Zhao, Y. J. Cui and W. J. Chen, *Polym. Int.*, 2020, **69**, 140–148.
- 27 P. S. Luan and G. S. Oehrlein, *Langmuir*, 2019, **35**, 4270–4277.
- 28 X. S. Duan, Y. L. Fang, X. Cheng, Z. L. Du, M. Zhou and H. B. Wang, *ACS Sustainable Chem. Eng.*, 2018, **6**, 15541–15549.
- 29 C. Hao, T. Liu, S. Zhang, W. C. Liu, Y. F. Shan and J. W. Zhang, *Macromolecules*, 2020, **53**, 3110–3118.



- 30 R. T. Pekarek, A. Affolter, L. L. Baranowski, J. Coyle, T. Z. Hou, E. Sivonxay, B. A. Smith, R. D. McAuliffe, K. A. Persson, B. Key, C. Apblett, G. M. Veith and N. R. Neale, *J. Mater. Chem. A*, 2020, **8**, 7897–7906.
- 31 Q.-A. Poutrel, J. J. Blaker, C. Soutis, F. Tournilhac and M. Gresil, *Polym. Chem.*, 2020, **11**, 5327–5338.
- 32 E. O. Kissi, H. Grohgan, K. Löbmann, M. T. Ruggiero, J. Axel Zeitler and T. Rades, *J. Phys. Chem. B*, 2018, **122**, 2803–2808.
- 33 A. K. Padhan and D. Mandal, *Polym. Chem.*, 2018, **9**, 3248–3261.
- 34 C. Ma, S. L. Qiu, B. Yu, J. L. Wang, C. M. Wang, W. R. Zeng and Y. Hu, *Chem. Eng. J.*, 2017, **322**, 618–631.
- 35 X. L. Wang, C. Santschi and O. JF Martin, *Small*, 2017, **13**, 1700044.
- 36 G. Zhou, X. Y. Zhang, S. L. Li, Y. Sun, F. C. Tian, C. C. Xu, Y. N. Miao and W. J. Jiang, *Constr. Build. Mater.*, 2021, **312**, 125310.
- 37 A. Hung and E. H. Fini, *ACS Sustainable Chem. Eng.*, 2020, **8**, 11764–11771.

